

Exact solution and magnetic properties of an anisotropic spin ladder

Zu-Jian Ying^{1,2,3}, Itzhak Roditi¹, Angela Foerster³, Bin Chen²

1. Centro Brasileiro de Pesquisas Físicas, Rua Dr. Xavier Sigaud 150, 22290-180 Rio de Janeiro, RJ, Brasil

2. Hangzhou Teachers College, Hangzhou 310012, China

3. Instituto de Física da UFRGS, Av. Bento Gonçalves, 9500, Porto Alegre, 91501-970, Brasil

()

We study an integrable two-leg spin-1/2 ladder with an XYZ-type rung interaction. Exact rung states and rung energies are obtained for the anisotropic rung coupling in the presence of a magnetic field. Magnetic properties are analyzed at both zero and finite temperatures via the thermodynamic Bethe ansatz and the high-temperature expansion. According to different couplings in the anisotropic rung interaction, there are two cases in which a gap opens, with the ground state involving one or two components in the absence of a magnetic field. We obtain the analytic expressions of all critical fields for the field-induced quantum phase transitions (QPT). Anisotropic rung interaction leads to such effects as separated magnetizations and susceptibilities in different directions, lowered inflection points and remnant weak variation of the magnetization after the last QPT.

I. INTRODUCTION

Recently the quasi-one-dimensional spin ladder has attracted much interest both experimentally and theoretically [1]. More and more ladder-structure compounds have been realized, such as SrCu_2O_3 [2], $\text{Cu}_2(\text{C}_5\text{H}_{12}\text{N}_2)_2\text{Cl}_4$ [3], $(5\text{IAP})_2\text{CuBr}_4 \cdot 2\text{H}_2\text{O}$ [4], $(\text{C}_5\text{H}_{12}\text{N})_2\text{CuBr}_4$ [5], and so forth. Although many ladder compounds can be well described by simple isotropic ladders, the structural distortion and the spin-orbital interaction of the transition ions can lead to various magnetic anisotropies. Besides the spin-orbital interaction, both on-site Coulomb exchange interaction [6,7] and nonlocal Coulomb interaction [8] also influence the anisotropy. Anisotropic interaction from bond buckling has been recently found in copper-oxide ladder compounds CaCu_2O_3 [9] due to an angle deviation from 180° in the Cu-O-Cu bond [9–11]. An anisotropic rung interaction was considered in Ref. [12] motivated by CaCu_2O_3 [9] and a two-leg spin ladder with an XXZ-rung interaction was derived in the presence of the Dzyaloshinskii-Moriya interaction and the Kaplan-Shekhtman-Entin-Wohlman-Aharony interactions. When the Cu-O-Cu bond is near 90° , the rung interaction is weak in the copper-oxide ladder. Spin anisotropy in the exchange interaction also exists in strongly-coupled ladder compounds such as $(\text{pipdH})_2\text{CuBr}_4$ [13]. On the other hand, real spin ladder compounds are usually described by the standard Heisenberg ladder model, which is not exactly soluble, turning the computation of the physical properties for the ground state (GS), the gap, the thermodynamical quantities and other relevant properties in the presence of temperature and magnetic fields, rather difficult. Usually, just numerical calculations and perturbative schemes can be applied. Recently it was shown that the integrable spin ladder model [14] can describe the properties of strongly-coupled spin ladder compounds when a rescaling parameter is introduced [15,16]. Therefore, it can be expected that integrable ladders with

anisotropic rung interactions can provide some meaningful information in the physics of anisotropies. In addition, anisotropic rung interactions also provide us with some more adjustable parameters that may be useful in fitting the experimental data of compounds.

In the present paper we shall consider the anisotropy in the rung interaction and the corresponding magnetic anisotropic effect by solving an integrable spin ladder with a general XYZ rung interaction. By means of the thermodynamical Bethe ansatz (TBA) and the high temperature expansion (HTE) [15,17,18], we investigate the influence of the anisotropic rung interaction on the quantum phase transitions (QPT) and the magnetic properties. The contents are arranged as follows: (i) In the second section we present the model and the exact rung-state basis in the presence of a magnetic field. Then the model is solved by the Bethe ansatz (BA) approach. (ii) The third section gives the TBA equations for the GS and the HTE for physical properties at finite temperatures. (iii) In the fourth section, we study the field-induced QPT's. The rung anisotropy provides two kinds of gapped ladders, respectively with one and two components in the GS. The analytic expressions are obtained for all the critical fields of the corresponding QPT's. The rung anisotropy also leads to a separation of the magnetizations and susceptibilities in different directions. The magnetization inflection point (IP) may be lowered from the half-saturation and in the two-component gapped ladder the IP is even not invariant under different temperatures. A remnant variation of magnetization can be found after the last QPT. In the fifth section we give a summary of our results.

II. THE MODEL, EXACT RUNG STATES AND BA SOLUTION

We shall consider a spin-1/2 two-leg spin ladder model with a general XYZ-type anisotropy in the rung interac-

tion, whose Hamiltonian reads

$$\begin{aligned}
\mathcal{H} &= \mathcal{H}_0 + \mathcal{H}_{XYZ} + \mathcal{M}, \\
\mathcal{H}_0 &= \frac{J_0}{\gamma} \sum_{i=1}^L P_{i,i+1}, \\
\mathcal{H}_{XYZ} &= \sum_i (J_x S_i^x T_i^x + J_y S_i^y T_i^y + J_z S_i^z T_i^z), \\
\mathcal{M} &= -gH \sum_i (S_i^z + T_i^z), \tag{1}
\end{aligned}$$

where \vec{S} and \vec{T} are the spin operators for the two legs and g is the Landé g factor in the direction of the field. J_0 is the average of the leg interaction and γ is a rescaling parameter. The value $\gamma = 4$ was introduced in Refs. [16,15] in fitting with isotropic ladder compounds in the presence of weak rung. The bulk part \mathcal{H}_0 with the permutation operator $P_{i,i+1} = (2\vec{S}_i \cdot \vec{S}_{i+1} + \frac{1}{2})(2\vec{T}_i \cdot \vec{T}_{i+1} + \frac{1}{2})$ exhibits the SU(4) symmetry [19]. Isotropic integrable spin ladder [14] has identical J_x , J_y and J_z .

When the rung interaction is strong, it is favorable for the spin ladder system to form rung states, since the leg interaction is too weak to take apart the rung state. Anisotropy in the rung interaction leads to the collapse of the conventional singlet and triplet rung states from the isotropic ladder, even in the absence of the field. However, we find a new exact basis valid both in the absence and presence of an external magnetic field,

$$\begin{aligned}
\varphi_1 &= \frac{1}{\sqrt{2}} (|\uparrow\downarrow\rangle - |\downarrow\uparrow\rangle), & \varphi_2 &= \frac{1}{\sqrt{2}} (|\uparrow\downarrow\rangle + |\downarrow\uparrow\rangle) \\
\varphi_3 &= \frac{|\uparrow\uparrow\rangle - \eta^{-1} |\downarrow\downarrow\rangle}{\sqrt{1 + \eta^{-2}}}, & \varphi_4 &= \frac{|\uparrow\uparrow\rangle + \eta |\downarrow\downarrow\rangle}{\sqrt{1 + \eta^2}} \tag{2}
\end{aligned}$$

where

$$\eta^{\pm 1} = \frac{\pm 4gH + \sqrt{(4gH)^2 + (J_x - J_y)^2}}{J_x - J_y}. \tag{3}$$

Then the corresponding rung energies include the Zeeman energy in a nonlinear way,

$$\begin{aligned}
E_1 &= -\frac{1}{4}(J_x + J_y + J_z), \\
E_2 &= \frac{1}{4}(J_x + J_y - J_z), \\
E_3 &= -\sqrt{(gH)^2 + \frac{1}{16}(J_x - J_y)^2} + \frac{1}{4}J_z, \\
E_4 &= \sqrt{(gH)^2 + \frac{1}{16}(J_x - J_y)^2} + \frac{1}{4}J_z. \tag{4}
\end{aligned}$$

The rung states $\{\varphi_i \mid i = 1, \dots, 4\}$ provides a new fundamental representation of the SU(4) Lie algebra $S_m^n \varphi_i = \delta_{n,i} \varphi_m$ with commutation relations of the generators $[S_m^n, S_k^l] = \delta_{n,k} S_m^l - \delta_{m,l} S_k^n$. Based on this SU(4) realization and the vanishing commutation relations $[\mathcal{H}_{XYZ}, \mathcal{H}_0] = [\mathcal{M}, \mathcal{H}_0] = 0$, one can solve the

model (1) via the BA approach [20]. The BA equations are the same as those obtained for the SU(4) model [21] and for the SU(3) \otimes U(1) spin ladder [14]. Here we present the BA equations together with the eigenenergy

$$\begin{aligned}
-\prod_{m=1}^{M^{(k)}} \Xi_1(\mu_{j,m}^{k,k}) &= \prod_{m=1}^{M^{(k+1)}} \Xi_{\frac{1}{2}}(\mu_{j,m}^{k,k+1}) \prod_{m=1}^{M^{(k-1)}} \Xi_{\frac{1}{2}}(\mu_{j,m}^{k,k-1}), \\
E &= -\sum_{j=1}^{M^{(1)}} 2\pi a_1(\mu_j^{(1)}) + \sum_{i=1}^4 E_i N_i, \tag{5}
\end{aligned}$$

where $\Xi_x(\mu_{j,m}^{k,l}) = (\mu_j^{(k)} - \mu_m^{(l)} - xi)/(\mu_j^{(k)} - \mu_m^{(l)} + xi)$, $\mu_j^{(0)} = 0, M^{(0)} = L, M^{(4)} = 0$, and $1 \leq k \leq 3$; $a_n(\mu) = \frac{1}{2\pi} \frac{n}{\mu^2 + n^2/4}$. There are L rungs, N_i is the total number of rung state φ_i and $\mu_j^{(k)}$ is the rapidity. $M^{(k)}$ is the total rapidity number in the k 'th branch.

From the BA equations and the eigenenergy we can apply the TBA and HTE to study the collective properties of the model. When the field is applied in the x or y direction, one only needs to permute the anisotropy parameter values $\{J_x, J_y, J_z\}$ as well as the corresponding g factors. We incorporate g into the field unit in plotting figures to investigate the net effect of the anisotropic rung interaction. For a powder sample, a simple way is to take an average of the three directions.

III. TBA AND HTE

By adopting the string conjectures [22] and applying the Yang-Yang method [23] at the thermodynamic limit, one can obtain the GS equations for three dressed energies $\epsilon^{(i)}$,

$$\epsilon^{(i)} = g^{(i)} - a_2 * \epsilon^{(i)-} + a_1 * (\epsilon^{(i-1)-} + \epsilon^{(i+1)-}), \tag{6}$$

where $\epsilon^{(0)} = \epsilon^{(4)} = 0$ and the symbol $*$ denotes the convolution. The basis order is chosen as $(\varphi_{P_1} \varphi_{P_2} \varphi_{P_3} \varphi_{P_4})^T$, where $P_i \in \{1, 2, 3, 4\}$ and φ_{P_1} is energetically the most favorable state while φ_{P_4} is the least favorable one. For the chosen order the driving term is given by $g^{(i)} = E_{P_{i+1}} - E_{P_i}$. The GS is composed of Fermi seas filled by negative $\epsilon^{(i)-}$. If some branch of the dressed energy is all positive, then the corresponding excitations to this branch is gapful. A QPT occurs at the point where the gap is closed. We shall apply these TBA equations to analyze the field-induced QTP for the GS.

For the finite temperature case the TBA involves an infinite number of coupled integral equations. In the present paper we shall apply the HTE [18,17,15] from T-system [24] within the Quantum Transfer Matrix formalism [25], which involves only a finite number of integral equations and consequently is more convenient. Following Refs. [15,18,17], one can obtain the free energy f for per rung in high temperatures. Here we present

the first four terms which dominate the physics for high temperatures:

$$f = -T \left(C_0 + C_1 \left(\frac{J_0}{\gamma T} \right) + C_2 \left(\frac{J_0}{\gamma T} \right)^2 + C_3 \left(\frac{J_0}{\gamma T} \right)^3 \right) \quad (7)$$

where T is the temperature, the coefficients are

$$C_0 = \ln Q_+, \quad C_1 = \frac{2Q}{Q_+^2}, \quad C_2 = \frac{3Q}{Q_+^2} - \frac{6Q^2}{Q_+^4} + \frac{3Q_-}{Q_+^3},$$

$$C_3 = \frac{10Q}{3Q_+^2} - \frac{18Q^2}{Q_+^4} + \frac{80Q^3}{3Q_+^6} + \frac{8Q_-}{Q_+^3} - \frac{24QQ_-}{Q_+^5} + \frac{4}{Q_+^4},$$

with the definitions

$$Q = 2 \cosh\left(\frac{1}{2}\beta J_z\right) + 4 \cosh\left(\frac{1}{4}\beta J_{x+y}\right) \cosh(\beta h),$$

$$Q_{\pm} = 2e^{(\pm\beta J_z/4)} \cosh\left(\frac{1}{4}\beta J_{x+y}\right) + 2e^{(\mp\beta J_z/4)} \cosh(\beta h),$$

$h = \sqrt{(gH)^2 + J_{x-y}^2/16}$, $J_{x\pm y} = J_x \pm J_y$ and $\beta = 1/T$. One can get higher orders for lower temperatures. The magnetization and the susceptibility can be easily obtained by $M = -\partial f/\partial H$, $\chi = \partial M/\partial H$. The rescaling parameter $\gamma = 4$ in the isotropic case [16,15] gives the leading term of the gap for the integrable ladder in fitting with the experimental ladder compounds. If the rung J_0 is weak, then the HTE gives a valid result even for low temperatures due to the large rescaling γ .

IV. PHASE TRANSITIONS AND MAGNETIC PROPERTIES

A. One-component gapped ladder

For different anisotropies there are two different gapped ladders. In one case, only one component φ_1 exists in the gapped GS when $H = 0$. In the other case both φ_1 and φ_2 are involved in the gapped GS. First we discuss the former case which happens more likely. It requires

$$J_z + J_3 - |J_x - J_y| > 16J_0/\gamma, \quad (8)$$

$$J_x + J_y > 8J_0/\gamma, \quad (9)$$

where $J_3 = J_z + J_y + J_x$. Condition (8) expels the components φ_3 and φ_4 from the GS, while condition (9) excludes the component φ_2 . The field will bring φ_3 down to the ground state and close the gap $\Delta = \min\{E_2, E_3, E_4\} - E_1 - 4J_0/\gamma$ at a critical field H_{c1} , which leads to the first quantum phase transition (QPT). Further increase of the field will bring all components of φ_1 out of the GS and another gap $\Delta = E_1 - E_3 - 4J_0/\gamma$ opens at the critical field H_{c2} , which characterizes another QPT. The factor $4J_0/\gamma$ in the gap comes from the maximum depth of the first dressed energy branch. It is easy to see that only the components φ_1 and φ_3 compete

in the GS involving one branch of dressed energy, since the GS only consists of φ_1 in the absence of the field while only φ_3 is lowered in energy level when the field is applied. The analytic expressions of two critical fields can be obtained exactly as

$$H_{c1} = \frac{1}{2g} \sqrt{J_z J_3 + J_x J_y + 64 \left(\frac{J_0}{\gamma} \right)^2 - 8 \frac{J_0}{\gamma} (J_z + J_3)},$$

$$H_{c2} = \frac{1}{2g} \sqrt{J_z J_3 + J_x J_y + 64 \left(\frac{J_0}{\gamma} \right)^2 + 8 \frac{J_0}{\gamma} (J_z + J_3)}. \quad (10)$$

Setting $J_z = J_y = J_x$ recovers the result for isotropic case [16], as expected. A weak anisotropy will lead to different critical fields and consequently separate the magnetizations in different directions. We give an example of the magnetization with weak anisotropy in Fig.1, a low-temperature magnetization was presented for comparison in the z direction. The corresponding low-temperature magnetizations for all three directions are presented in Fig.2, obtained from the HTE. Magnetizations in different directions for strong anisotropy are demonstrated as an example in Fig.3 for the GS and in Fig.4 for a low temperature.

Before the gap is closed at H_{c1} , the gap Δ near H_{c1} can be expanded to a simpler form

$$\Delta \cong c_1 (H_{c1} - H), \quad (11)$$

$c_1 = g^2 H_{c1} / \sqrt{(gH_{c1})^2 + \frac{1}{16}(J_x - J_y)^2}$. Considerable excitations can be stimulated by the temperature T if T is in the order of the gap $T \sim (H_{c1} - H)$, the magnetization will rise from zero before the field reaches the critical point. An expansion based on small Fermi points [16] gives the zero-temperature critical behavior in the vicinity of H_{c1}

$$\langle M^z \rangle \cong \langle M^z \rangle_3 \frac{1}{\pi} \sqrt{\frac{c_1}{J_0/\gamma}} (H - H_{c1})^{1/2}. \quad (12)$$

Here $\langle M^z \rangle_3$ is the magnetization of a single rung state φ_3 , it also varies with the field due to the anisotropic rung interaction, as we will discuss below in (17). For the lowest order in the critical behavior, $\langle M^z \rangle_3$ takes the value at the critical point H_{c1} . This $M^z \propto (H - H_{c1})^{1/2}$ critical behavior, typical for gapped integer spin antiferromagnetic chains [26], is buried by the afore-mentioned temperature effect. This temperature effect can be seen in Fig.5, in which the magnetization of the z direction at $T = 0.5J_0$ becomes considerable at the field $H = H_{c1} - 0.5J_0$. Actually the magnetization at $T = 0.5J_0$ increases nearly in a linear way before the H_{c1} .

A special point in the magnetization is the inflection point (IP) H_{IP} , which is an invariant point under low temperatures,

$$gH_{IP} = \frac{1}{2} \sqrt{(J_z + J_x)(J_z + J_y)} \quad (13)$$

where the two components φ_1 and φ_3 have the same rung energies $E_1 = E_3$ and the same proportion $N_1 = N_3$ in the GS. The excitations to φ_2 and φ_4 are gapful, the gap can be obtained exactly from (6)

$$\begin{aligned}\Delta_{IP} &= \min\{\Delta_{IP2}, \Delta_{IP4}\}, \\ \Delta_{IP2} &= (J_x + J_y)/2 - (2 \ln 2)J_0/\gamma, \\ \Delta_{IP4} &= (J_z + J_3)/2 - (2 \ln 2)J_0/\gamma.\end{aligned}\quad (14)$$

At low temperatures, the excitations to φ_2 or φ_4 are difficult to stimulate, while the temperature does not influence the relative proportion between φ_1 and φ_3 due to their same energies at the IP. Consequently the proportions of φ_1 and φ_3 remain almost unchanged when the temperature varies. Therefore the magnetization at H_{IP} also remains unmoved when the temperatures changes, and the magnetization curves of various temperatures cross each other at the same point M_{IP} , which is shown by the curves for temperatures $T = 0, 0.5J_0, 0.75J_0$ and J_0 in Fig.5. This requires low temperatures

$$T \ll \Delta_{IP} \quad (15)$$

as well as the gapped ladder conditions (8) and (9), Δ_{IP} is the excitation gap to φ_2 or φ_4 in (14). When the temperature is sufficiently high such that the excitations to φ_2 or φ_4 are considerable, the involvement of these components reduces the proportion of φ_3 which has the highest magnetization. The components φ_2 and φ_4 have zero and negative magnetizations, respectively. As a result, the magnetization at H_{IP} deviates from M_{IP} and move downwards. We show this moving by magnetization curves at temperatures $T = 10J_0, 20J_0$ in Fig.5, for which one can find observation examples in $\text{Cu}_2(\text{C}_5\text{H}_{12}\text{N}_2)_2\text{Cl}_4$ [3].

The magnetization at the IP can be worked out as

$$M_{IP}^z = \frac{g H_{IP}^2 + H_{IP}H_{IP}^{(+)}}{2 H_{IP}^{(+2)} + H_{IP}H_{IP}^{(+)}} \quad (16)$$

where $H_{IP}^{(+)} = \sqrt{H_{IP}^2 + (J_x - J_y)^2/(4g)^2}$. For the isotropic ladder, $H_{IP}^{(+)} = H_{IP}$ and consequently M_{IP}^z is located at the half of the saturation magnetization $M_s^z = g$ [15]. The anisotropy lowers the magnetization of the IP due to $H_{IP}^{(+)} > H_{IP}$, i.e. $M_{IP}^z/M_s^z < 1/2$. Physically, the anisotropy in x, y directions hybridizes the elemental state $|\downarrow\downarrow\rangle$ into φ_3 so that φ_3 is not a pure fully-polarized elemental state $|\uparrow\uparrow\rangle$ as in the isotropic case. For XXZ-type rung interaction M_{IP}^z is half-saturation when the field is oriented in z direction, but also lowered when the field is applied in other directions. This IP lowering effect is more obvious for the strong anisotropic case, we give an example in Fig.3. As one can see from this figure, besides the strong separation of the magnetization in different directions, the IP points in x and z directions move below the half saturation point.

In addition to the separation of the magnetization in different directions and the lowering of the inflection

points, another property in the anisotropic case is the remnant variation of the magnetization after the second phase transition. The fact that magnetization increases between H_{c1} and H_{c2} mainly comes from the proportional competition between the two state φ_1 and φ_3 , i.e., more rungs are occupied by φ_3 when the field gets higher. The single-rung magnetization in state φ_3 can be obtained explicitly

$$\langle M^z \rangle_3 = g \frac{\eta^2 - 1}{\eta^2 + 1}, \quad (17)$$

where η increases with the field from the expression (3). The long-dashed line in Fig.3 gives an example of $\langle M^z \rangle_3$ in z direction, which increases from zero from the beginning of the application of the magnetic field. If H_{c1} is small, then the increment of $\langle M^z \rangle_3$ also contributes with an important part to the growth of the magnetization. Otherwise for higher H_{c1} , the change of $\langle M^z \rangle_3$ contributes less to the growth of the total magnetization, since $\langle M^z \rangle_3$ has slowed down in increasing before the first quantum phase transition occurs. However, the competition between φ_1 and φ_3 comes to end after the second phase transition and the magnetization is completely $\langle M^z \rangle_3$. This gives a remnant variation of magnetization even after the second phase transition, since $\langle M^z \rangle_3$ is still approaching to the saturation limit. This remnant variation of magnetization is illustrated for the ground state in Fig.3 and can also be seen for the temperature case (Fig.4).

Examples of the magnetic susceptibility in the three directions are plotted in Fig.6 for weakly anisotropic rung and in Fig.7 for strongly anisotropic rung. Weak anisotropy separates the heights of the magnetic susceptibility peak, while a strong anisotropy also leads to an obvious separation of the whole susceptibility including the peak positions.

B. Two-component gapped ladder

Anisotropy in the rung interaction also provides another possibility of a gapped ladder, in which not only the rung state φ_1 but also φ_2 are involved in the GS before the field is applied and brings about the first QPT. The single-state energy difference is $E_2 - E_1 = (J_x + J_y)/2$. The larger is the difference, the more strongly φ_1 and φ_2 will expel each other in the Fermi sea. The two-component gapped ladder requires

$$|J_x + J_y| < 8J_0/\gamma, \quad (18)$$

so that φ_1 and φ_2 are close enough in the energy levels to exist in the GS at the same time in the absence of the field. Also a strong J_z is needed to expel φ_3 and φ_4 from the gapped GS before the field is applied, approximately

$$J_z > 4 \ln 2 \frac{J_0}{\gamma} + \frac{1}{2} |J_x - J_y| + \frac{\gamma}{8\pi^2 J_0} (J_x + J_y)^2. \quad (19)$$

For simplicity, we assume $J_x + J_y > 0$ so that φ_1 has lower energy than φ_2 , one only needs to change $J_x + J_y$ to be $-(J_x + J_y)$ for lower φ_2 . The first QPT occurs when the field brings down φ_3 and gets involved in the GS, the critical field can be obtained with the help of the Wiener-Hopf technique [27] which is valid for large Fermi points (Fermi surface in one dimension). Explicitly we have

$$gH_{c1} \cong \sqrt{\left[\frac{J_z}{2} - 2 \ln 2 \frac{J_0}{\gamma} - \frac{(J_x + J_y)^2}{16\pi^2 J_0/\gamma}\right]^2 - \frac{(J_x - J_y)^2}{16}}, \quad (20)$$

which gives a good approximation if the value of $J_x + J_y$ is not very close to $8J_0/\gamma$. Further increase will lower the energy of φ_3 below φ_1 and φ_2 and bring them out of the GS one by one. The component variations in the QPT are $\{\varphi_1, \varphi_2\} \rightarrow \{\varphi_1, \varphi_2, \varphi_3\} \rightarrow \{\varphi_1, \varphi_3\} \rightarrow \{\varphi_3\}$, where each arrow indicates the occurrence of a QPT. Since φ_2 has also zero magnetization, the total magnetization also remains null in the gapped phase before the first QPT. The zero-magnetization component φ_2 gets out of the GS after H_{IP} if

$$J_x + J_y < (4 \ln 2)J_0/\gamma, \quad (21)$$

while for

$$(4 \ln 2)J_0/\gamma < J_x + J_y < 8J_0/\gamma, \quad (22)$$

φ_2 is brought off the GS before H_{IP} . These happen at the second QPT with an approximate critical field

$$gH_{c2} \cong \sqrt{\left[\frac{1}{2}J_z - \frac{3}{4}J_{x+y} + 4 \ln 2 \frac{J_0}{\gamma} + \frac{\delta^2 \gamma}{2\pi^2 J_0}\right]^2 - \frac{J_{x-y}^2}{16}}, \quad (23)$$

where $\delta = J_{x+y} - 4 \ln 2(J_0/\gamma)$. The expression (23) can give a satisfactory approximation when the value of $|\delta|$ is not near $4J_0/\gamma$. The exact critical field H_{c3} for the third QPT is the same as H_{c2} in (10). When the example in fig.(8) has numerical points $H_{c1} = 1.061J_0$ and $H_{c2} = 1.232J_0$, the expressions (20) and (23) provide analytic results $H_{c1} = 1.064J_0$ and $H_{c2} = 1.231J_0$.

The IP in the one-component gapped ladder case will not be invariant in the two-component ladder case. If the component φ_2 gets out of the GS after H_{IP} , the φ_2 is gapless. Although the components φ_1 and φ_3 still have the same proportion at the IP, any small temperature will excite more components of φ_2 and consequently decreases the proportion of φ_1 and φ_3 . Therefore the temperature will lower the total magnetization from that of the GS. If the component φ_2 gets out of the GS before H_{IP} , with the condition (22), the IP is hardly an invariant. Despite of the existence of a gap for excitations to φ_2 at H_{IP} , the gap is actually quite small

$$\Delta_{IP2} < (4 - \ln 2)J_0/\gamma, \quad (24)$$

relative to the strong rung interaction. So a low temperature of order J_0 will still stimulate considerable excitations to φ_2 and lower the magnetization at H_{IP} . We illustrate this by an example in Fig.(8).

V. SUMMARY

We have introduced a two-leg spin-1/2 ladder with a general anisotropic XYZ rung interaction. In particular, the exact rung state basis for this model was found. We have studied the effect of the anisotropic rung interaction by solving the integrable ladder in the context of the thermodynamical Bethe ansatz and the high-temperature expansion. Two kinds of gapped ladders were provided, respectively involving one and two components in the GS in the absence of the magnetic field. We have obtained analytically all the corresponding critical fields for the field-induced quantum phase transitions. The magnetizations and susceptibilities in different directions separates under the rung anisotropy. The magnetization inflection point is lowered from the half-saturation and a weak changing in magnetization still remains after the last quantum phase transition. The inflection point in the two-component gapped ladder case is not invariant as in the one-component gapped ladder case due to field-deduced three-component competition or small excitation gap.

ACKNOWLEDGMENTS

We thank Huan-Qiang Zhou and Xi-Wen Guan for helpful discussions. ZJY thanks FAPERJ and FAPERGS for financial support. IR thanks PRONEX and CNPq. AF thanks FAPERGS and CNPq. BC is supported by National Nature Science Foundation of China under Grant No.10274070 and Zhejiang Natural Science Foundation RC02068.

-
- [1] E. Dagotto and T. M. Rice, Science **271**, 618 (1996); E. Dagotto, Rep. Prog. Phys. **62**, 1525 (1999).
 - [2] M. Azuma, Z. Hiroi, M. Takano, K. Ishida and Y. Kitaoka, Phys. Rev. Lett. **73**, 3463 (1994).
 - [3] G. Chaboussant, P. A. Crowell, L. P. Lévy, O. Piovesana, A. Madouri, and D. Mailly, Phys. Rev. B **55**, 3046 (1997).
 - [4] C. P. Landee, M. M. Turnbull, C. Galeriu, J. Giantsidis, and F. M. Woodward, Phys. Rev. B **63**, 100402 (2001).
 - [5] B. C. Watson, V. N. Kotov, M. W. Meisel, D. W. Hall, G. E. Granroth, W. T. Montfrooij, S. E. Nagler, D. A. Jensen, R. Backov, M. A. Petruska, G. E. Fanucci, and D. R. Talham, Phys. Rev. Lett. **86**, 5168 (2001).
 - [6] T. Yildirim, A. B. Harris, O. Entin-Wohlman, and A. Aharony, Phys. Rev. Lett. **73**, 2919 (1994).

- [7] J. Stein, O. Entin-Wohlman, and A. Aharony, Phys. Rev. B **53**, 775 (1996).
- [8] T. Moriya, Phys. Rev. **120**, 91 (1960); J. Stein, Phys. Rev. B **53**, 785 (1996).
- [9] V. Kiryukhin, Y. J. Kim, K. J. Thomas, F. C. Chou, R. W. Erwin, Q. Huang, M. A. Kastner and R. J. Birgeneau, Phys. Rev. B **63**, 144418 (2001).
- [10] V.Yu. Yushankhai and R. Hayn, Europhys. Lett. **47**, 116 (1999).
- [11] V. Kataev, K.-Y. Choi, M. Grüninger, U. Ammerahl, B. Büchner, A. Freimuth, A. Revcolevschi, Physica B **312-313**, 614 (2002).
- [12] R. Citro and E. Orignac, Phys. Rev. B **65**, 134413 (2002).
- [13] B.R. Patyal, B.L. Scott, and R.D. Willett, Phys. Rev. B **41**, 1657 (1990).
- [14] Y. Wang, Phys. Rev. B **60**, 9236 (1999).
- [15] M. T. Batchelor, X.-W. Guan, N. Oelkers, K. Sakai, Z. Tsuboi, and A. Foerster, Phys. Rev. Lett. **91**, 217202 (2003).
- [16] M.T. Batchelor, X.W. Guan, A. Foerster and H.Q. Zhou, New J. Phys. **5**, 107 (2003).
- [17] Z. Tsuboi, J. Phys. A **36**, 1493 (2003).
- [18] M. Shiroishi and M. Takahashi, Phys. Rev. Lett. **89**, 117201 (2002).
- [19] Y.Q. Li, M. Ma, D.N. Shi and F.C. Zhang, Phys. Rev. Lett. **81**, 3527 (1998).
- [20] B. Sutherland, Phys. Rev. B **12**, 3795 (1975).
- [21] Y.Q. Li, M. Ma, D.N. Shi and F.C. Zhang, Phys. Rev. B **60**, 12781 (1999).
- [22] M. Takahashi, Prog. Theor. Phys. **46**, 401 (1971).
- [23] C.N. Yang and C.P. Yang, J. Math. Phys. **10**, 1115(1969).
- [24] A. Kuniba, T. Nakanishi, and J. Suzuki, Int. J. Mod. Phys. A **9**, 5215 (1994).
- [25] M. Suzuki, Phys. Rev. B **31**, 2957 (1985); A. Klümper, Ann. Phys. (Leipzig) **1**, 540 (1992); G. Jüttner, A. Klümper, and J. Suzuki, Nucl. Phys. B **487**, 650 (1997).
- [26] I. Affleck, Phys. Rev. B **43**, 3215 (1991).
- [27] M.G. Krein Usp. Mat. Nauk **13**, 3 (1958).

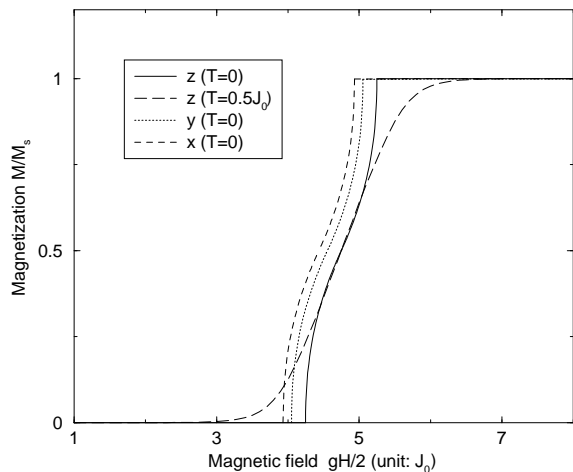


FIG. 1. Magnetization versus the magnetic field at zero temperature for the one-component gapped ladder with a weakly-anisotropic rung interaction, $J_x = 8J_0$, $J_y = 9J_0$, $J_z = 10.5J_0$, with the rescaling $\gamma = 4$. M_s is the saturation magnetization. In the gapped phase $H < H_{c1}$, only one component φ_1 exists in the ground state. To study the net effect of the anisotropic rung interaction, we incorporate the g factor into the field. The weak anisotropy in the rung separates the magnetization in different directions. The zero temperature magnetization is obtained from the thermodynamical Bethe ansatz (TBA). Also for comparison with the finite temperature case, a magnetization at $T = 0.5J_0$ obtained from the high-temperature expansion (HTE) is presented in the z direction.

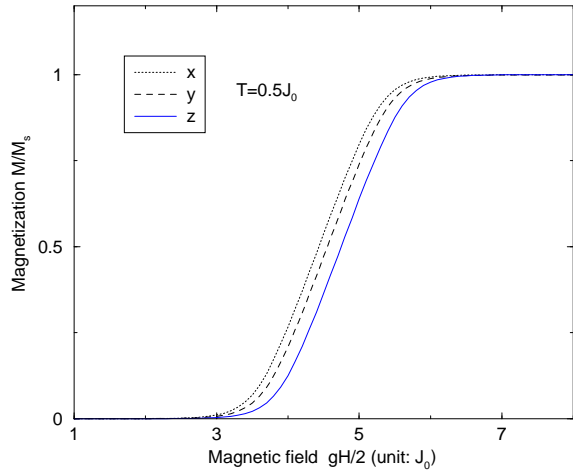


FIG. 2. Magnetization versus the magnetic field for $T = 0.5J_0$ for the one-component gapped ladder with the weak anisotropy, $J_x = 8J_0$, $J_y = 9J_0$, $J_z = 10.5J_0$ and $\gamma = 4$. The magnetizations are obtained from the HTE, which coincides with the magnetization separation in the zero temperature case obtained from the TBA.

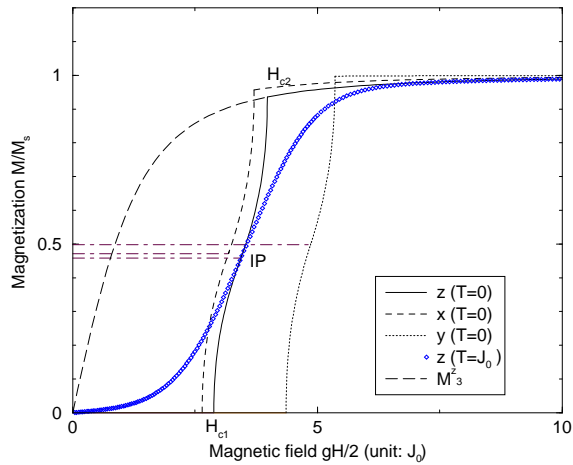


FIG. 3. Magnetization versus the magnetic field at zero temperature for the one-component gapped ladder with a strongly-anisotropic rung interaction, $J_x = 3J_0$, $J_y = 15J_0$, $J_z = 6J_0$, $\gamma = 4$. The strong anisotropy leads to a strong separation of the magnetization. The inflection point (IP) is lowered from the half saturation. A temperature magnetization from HTE is present to demonstrate the IP. Note that the magnetizations do not reach the saturation after the second quantum phase transition at H_{c2} , there still remains a weak variation of magnetizations. This remnant magnetization variation comes from the single-state magnetization M_3^z of φ_3 which is a mixture of full-polarized states $|\uparrow\uparrow\rangle$ and the lowest-magnetized state $|\downarrow\downarrow\rangle$. The variation of M_3^z is illustrated by the long-dashed line for the whole process of the field application.

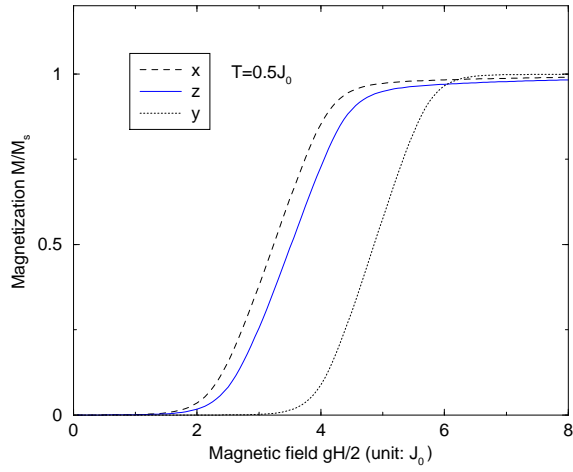


FIG. 4. Magnetizations versus the magnetic field for different directions in temperature case for the one-component gapped ladder with the strong anisotropy, $J_x = 3J_0$, $J_y = 15J_0$, $J_z = 6J_0$, $\gamma = 4$.

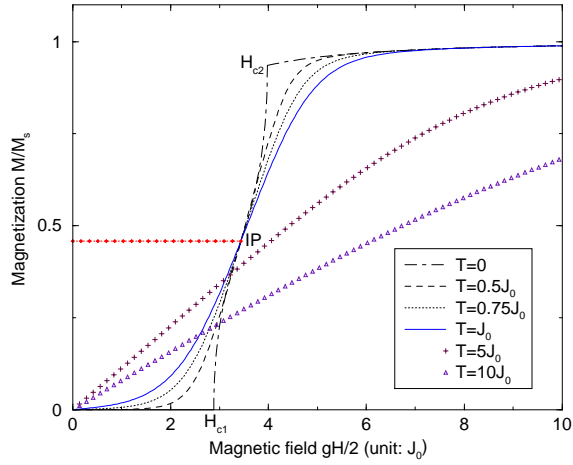


FIG. 5. Magnetization versus the magnetic field at different temperatures for the strongly-anisotropic rung, $J_x = 3J_0$, $J_y = 15J_0$, $J_z = 6J_0$, $\gamma = 4$. Low temperature magnetizations in $T = 0, 0.5J_0, 0.75J_0$ and J_0 cross the inflection point (IP). Higher-temperature magnetizations at $T = 5J_0$ and $10J_0$ do not go through the IP, as the gap for excitation to φ_2 is overcome by the temperature stimulation.

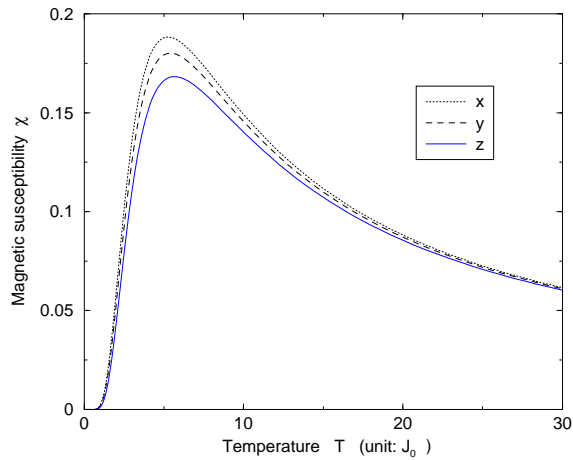


FIG. 6. Magnetic susceptibility against the temperature in different directions for the weakly-anisotropic case, $J_x = 8J_0$, $J_y = 9J_0$, $J_z = 10.5J_0$ and $\gamma = 4$. The weak anisotropy separate the heights of the susceptibility peaks. To see the net effect of the rung anisotropy, we plot the figures using the same g factors for the three directions.

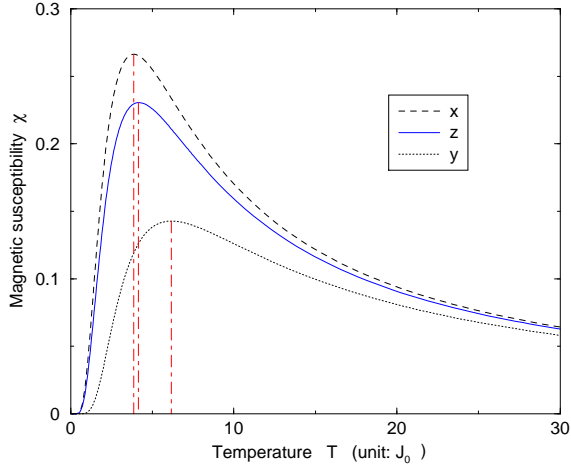


FIG. 7. Magnetic susceptibility versus the temperature in the strongly-anisotropic case, $J_x = 3J_0$, $J_y = 15J_0$, $J_z = 6J_0$, $\gamma = 4$. The strong anisotropy separate not only the peak heights but also the whole shape including the peak positions.

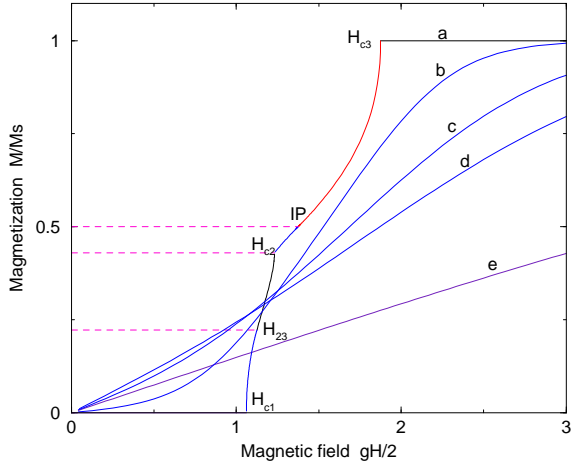


FIG. 8. Magnetizations in z direction of a two-component gapped ladder case, $J_x = J_y = 0.5J_0$, $J_z = 5J_0$, $\gamma = 4$. The curves a , b , c , d and e are plotted in different temperatures, respectively, $T = 0, 0.5J_0, J_0, 1.5J_0$ and $5J_0$. In the gapped phase $H < H_{c1}$, two components φ_1 and φ_2 involve in the ground state (GS) ($T=0$). The component φ_3 begins to enter the GS at the critical point H_{c1} and reaches the same energy as φ_2 at H_{23} . The component φ_2 get out of the GS at the second critical field H_{c2} . The magnetization curves of temperatures do not go through the IP as in the one-component gapped ladder case. When the field is applied in x or y direction the GS magnetization will increase from the beginning due to the gapless excitation in these directions.